

Exhibit 5

This Page Is Inserted by IFW Operations  
and is not a part of the Official Record

## **BEST AVAILABLE IMAGES**

Defective images within this document are accurate representations of the original documents submitted by the applicant.

Defects in the images may include (but are not limited to):

- BLACK BORDERS
- TEXT CUT OFF AT TOP, BOTTOM OR SIDES
- FADED TEXT
- ILLEGIBLE TEXT
- SKEWED/SLANTED IMAGES
- COLORED PHOTOS
- BLACK OR VERY BLACK AND WHITE DARK PHOTOS
- GRAY SCALE DOCUMENTS

**IMAGES ARE BEST AVAILABLE COPY.**

**As rescanning documents *will not* correct images,  
please do not report the images to the  
Image Problem Mailbox.**

E-5

# Dopamine neurons derived from embryonic stem cells function in an animal model of Parkinson's disease

Jong-Hoon Kim\*, Jonathan M. Auerbach\*†, José A. Rodríguez-Gómez, Iván Velasco, Denise Gavin, Nadya Lumelsky, Sang-Hun Lee†, John Nguyen†, Rosario Sánchez-Pernaute†, Krys Bankiewicz† & Ron McKay

Laboratory of Molecular Biology, National Institute of Neurological Disorders and Stroke, National Institute of Health, Bethesda, Maryland 20892, USA

\* These authors contributed equally to this work

Parkinson's disease is a widespread condition caused by the loss of midbrain neurons that synthesize the neurotransmitter dopamine. Cells derived from the fetal midbrain can modify the course of the disease, but they are an inadequate source of dopamine-synthesizing neurons because their ability to generate these neurons is unstable. In contrast, embryonic stem (ES) cells proliferate extensively and can generate dopamine neurons. If ES cells are to become the basis for cell therapies, we must develop methods of enriching for the cell of interest and demonstrate that these cells show functions that will assist in treating the disease. Here we show that a highly enriched population of midbrain neural stem cells can be derived from mouse ES cells. The dopamine neurons generated by these stem cells show electrophysiological and behavioural properties expected of neurons from the midbrain. Our results encourage the use of ES cells in cell-replacement therapy for Parkinson's disease.

Fetal midbrain precursors can proliferate and differentiate into dopamine-synthesizing neurons *in vitro*, and transplantation of these cells leads to recovery in a rat model of Parkinson's disease<sup>1,2</sup>. However, these precursor cells, which are derived from either rodent or human midbrain, generate dopamine neurons for only short periods in culture. ES cells can proliferate extensively in an undifferentiated state and may provide an unlimited source of many cell types. A related benefit of using ES cells is their accessibility for genetic engineering, which will permit the isolation and functional analysis of specific cell types. The isolation of human ES cells and the related embryonic germ cells has stimulated interest in their potential clinical value<sup>3,4</sup>. Although the use of ES cells in cell therapy is widely discussed, there are few cases showing that ES cell technology can be successfully applied to animal models of disease<sup>5-7</sup>. We have defined signals that improve the efficiency of dopamine-neuronal differentiation from ES cells, but this approach may still provide too few neurons for widespread use<sup>8</sup>. The purpose of our study here was to develop a method of further increasing the efficiency of midbrain-specific generation of dopamine neurons from ES cells, and to demonstrate that these cells can functionally integrate into host tissue as well as lead to recovery in a rodent model of Parkinson's disease.

## Generation of midbrain CNS precursors

Previously, we developed a five-stage method that leads to the efficient differentiation of ES cells into neurons<sup>8,9</sup>. Nuclear receptor related-1 (Nurr1) is a transcription factor that has a role in the differentiation of midbrain precursors into dopamine neurons<sup>10-13</sup>. We used a cytomegalovirus plasmid (pCMV) driving expression of a rat Nurr1 complementary DNA modified to express an antigenic site derived from the haemagglutinin protein (HA) to establish stable Nurr1 ES cell lines. Nurr1 ES cells were processed through the five-stage differentiation method<sup>8</sup>. Immunoblotting was used in stages 4 and 5 using anti-Nurr1 or anti-HA antibodies. The anti-HA

antibody shows that the introduced gene is expressed at high levels at stage 4 but at much lower levels at stage 5. In contrast, the endogenous Nurr1 gene was expressed at low levels in stage 4 cells but at higher levels after differentiation at stage 5 (Fig. 1a). These cells differentiated appropriately to cells positive for tyrosine hydroxylase (TH) (Fig. 1a and b). The subcellular localization of Nurr1 was monitored by immunocytochemistry using anti-HA antibody. In undifferentiated ES cells, Nurr1 was located in a restricted site in the nucleus (Fig. 1c). To assess whether Nurr1 induces TH expression in the appropriate neural cell types, we used double labelling for TH and specific molecular markers for neurons and glia. All TH<sup>+</sup> cells were double labelled with the neuronal marker TuJ1 but not with the markers for glial lineages (data not shown), indicating that the expression of the Nurr1 gene induced TH expression specifically in neurons. We found no evidence of elevated rates of cell death in Nurr1-expressing ES or neural stem cells (data not shown), ruling out that expression of transfected Nurr1 alters the distribution of cell fates by causing the death of specific cell types. Also, Nurr1 expression alone could not switch the regional identity of central nervous system (CNS) precursors, as evidenced by the lack of Engrailed 1 (En-1) expression in Nurr1-transfected cortical CNS stem cells positive for Bf1 (a forebrain-specific marker) (data not shown). These results suggest that the TH<sup>+</sup> neurons derived from Nurr1 ES cells are generated from precursor cells that are readily responsive to the actions of the Nurr1 protein.

Modification of the above procedure can differentiate ES cells into insulin-secreting structures similar to pancreatic islets<sup>14</sup>. This directly raises the important problem of enriching for specific cell types when using ES cells as a starting point. Cells at early stages of vertebrate development are thought to adopt mesodermal and ectodermal differentiation paths as alternate fates. Leukaemia inhibitory factor (LIF) inhibits the formation of cardiac mesoderm<sup>15</sup> and may promote neuronal differentiation at early stages of CNS development<sup>16</sup>. The pancreatic and duodenal homeobox-1 (Pdx-1) gene is an early regulator of the differentiation of cells in the endocrine pancreas<sup>17</sup>. LIF treatment of stage 2 cell aggregates strongly reduces the expression of Pdx-1 and promotes the differentiation of neurons.

† Present addresses: NeuralStem, Inc., 205 Perry Parkway, Gaithersburg, Maryland 20877, USA (J.M.A.); Department of Biochemistry, College of Medicine, Hanyang University, 133-791 Seoul, Korea (S.-H.L.); Department of Neurosurgery, University of California, San Francisco, California 94103, USA (J.N., K.B.); Neuroregeneration Laboratory, Harvard Medical School, McLean Hospital, Belmont, Massachusetts 02478, USA (R.S.-P.).

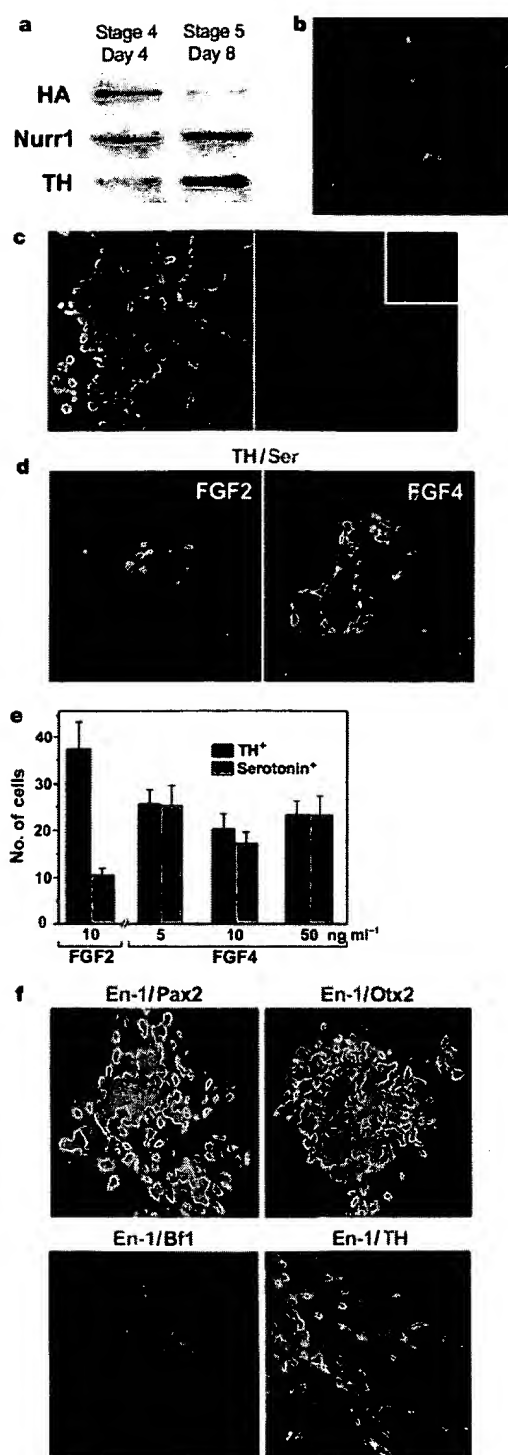


**Figure 1** Properties of neural precursors derived from Nurr1 ES cells. **a**, Immunoblot analysis for transfected Nurr1 (HA), total Nurr1 and TH at the end of stage 4 and at day 8 of stage 5. **b**, Differentiation of Nurr1-transfected ES cells into TH<sup>+</sup> (red) and serotonin<sup>+</sup> (green) neurons at day 10 of stage 5. The proportion of TH<sup>+</sup> cells was greater than that in wild-type ES cells. **c**, Nurr1 overexpression was evaluated using anti-HA immunostaining (red) at stage 1. DAPI (4,6-diamidino-2-phenylindole), blue; TH, green. Inset, co-localization of Nurr1 with DAPI at higher magnification. **d**, Stage 4 cells were cultured in the presence of Shh (500 ng ml<sup>-1</sup>) and FGF8 (100 ng ml<sup>-1</sup>) with 20 ng ml<sup>-1</sup> of FGF2 or FGF4 (5, 10 and 50 ng ml<sup>-1</sup>) and immunostained with TH and serotonin at day 10 of stage 5. **e**, The yield of TH<sup>+</sup> and serotonin<sup>+</sup> neurons/ low power field (SEM from 40 different fields of view). **f**, Nurr1-expressing stage 4 cells show markers of midbrain precursors. En-1<sup>+</sup> immunoreactivity co-localizes with Pax2 and Otx2. In contrast, few Bf1<sup>+</sup> cells were positive for En-1. After differentiation at stage 5, most TH<sup>+</sup> neurons expressed the midbrain-specific marker En-1.

In the developing CNS, midbrain dopamine-producing and hindbrain serotonin-producing neurons are generated on either side of the isthmus organizer, a signalling centre known to influence neuronal differentiation<sup>18,19</sup>. Both of these neuronal types are dependent on fibroblast growth factor 8 (FGF8) and sonic hedgehog (Shh) synthesized by the isthmus organizer<sup>18,19</sup>. In addition, precursors for serotonin-positive neurons in the ventral hindbrain are sensitive to FGF4 (ref. 20). The number of dopamine neurons generated from ES cells can be significantly increased when treating cells with FGF8 and Shh<sup>8</sup>. Therefore, we assessed the ability of FGF4 to generate serotonin neurons from ES cells by substituting FGF2 with FGF4 during stage 4. Stage 4 cells treated with FGF4 for 2 days and exposed to Shh and FGF8 for a further 4 days were analysed by immunocytochemistry after differentiation in stage 5 (Fig. 1d). FGF4 promoted a 2.5-fold increase in serotonin neurons and reduced the population of TH<sup>+</sup> cells (Fig. 1e). This result indicates that, as with endogenous mid- and hindbrain CNS precursors, the cell population at stage 4 is responsive to developmentally appropriate signals generated by the isthmus organizer.

To further define the cells present at stage 4, we evaluated the expression of transcription factors that characterize precursors in different regions of the CNS. Previous studies have shown that Otx2 expression occurs in the fore- and midbrain with a posterior limit at the isthmus organizer<sup>21,22</sup>. Pax2 is expressed in the mid- and hindbrain before becoming restricted to hindbrain cells<sup>21,22</sup>. At

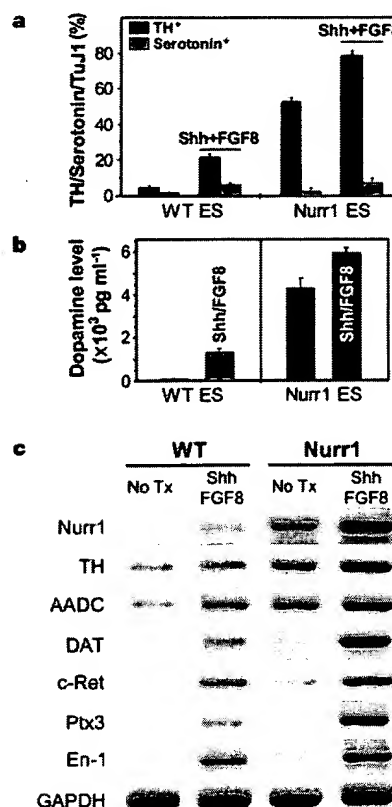


**Figure 2** Characterization of TH<sup>+</sup> neurons derived from Nurr1-transfected ES cells. **a**, Wild-type (WT) and Nurr1 ES cells were induced to differentiate by the five-stage protocol described in the text. The generation of TH<sup>+</sup> and serotonin<sup>+</sup> neurons was measured at day 10 of stage 5. The generation of TH<sup>+</sup> neurons is enhanced in wild-type and Nurr1 ES cells by treatment with Shh and FGF8 in stage 4. **b**, HPLC quantification of dopamine release by stage 5 ES cells after depolarization in HBSS (56 mM KCl) for 15 min. Data are shown as mean ± s.e.m. **c**, Expression analysis of genes involved in midbrain neuron development and function by RT-PCR in stage 5. Note that midbrain-specific genes *Nurr1*, *Ptx3*, *En-1* and the dopamine transporter (*DAT*) are expressed at low levels in the absence of Nurr1 overexpression and Shh/FGF8 treatment at stage 4.

stage 4, many cells positive for En-1 co-express Pax2 (65.5%) and Otx2 (80%) (Fig. 1f). Less than 1% of the En-1<sup>+</sup> cells label with Bf1 (ref. 23 and Fig. 1f). No cells expressing motor neuron transcription factors HB9 or Isl1 were seen at either stage 4 or 5 (data not shown). Also, similar to En-1 expression patterns seen in postmitotic differentiated dopamine neurons<sup>10,24</sup>, nearly all ES-derived TH<sup>+</sup> neurons expressed En-1 in their nucleus (Fig. 1f). These results strongly support the view that midbrain precursors and differentiated neurons can be efficiently generated from ES cells.

### Functional characterization of dopamine neurons

In ES cells, Nurr1 overexpression alone promoted an increase in the proportion of TH<sup>+</sup> neurons from 5 to 50% (Fig. 2a). When Shh and FGF8 were present at stage 4, the proportion of TH<sup>+</sup> neurons generated from Nurr1 ES cells could be increased to 78% (mean  $\pm$  s.e.m.,  $78.2 \pm 3.2$ ; Fig. 2a). In Nurr1 ES cells, serotonin-positive neurons were increased 2.3-fold by the treatment of Shh and FGF8, but this value is not significantly different from that in wild-type (WT) ES cells, indicating that the differentiation of serotonin neurons was not affected by Nurr1 (Fig. 2a). This is consistent

with *in vivo* data showing that deletion of Nurr1 has no effect on the serotonin neurons<sup>13</sup> and emphasizes that Nurr1 must act cooperatively with other signals specifically found in midbrain cells.

The capacity of the TH<sup>+</sup> neurons to synthesize and release dopamine was assessed by reverse-phase high-performance liquid chromatography (HPLC). The dopamine released by depolarization was markedly elevated in the cultures of stage 5 Nurr1 ES cells compared with WT ES cells (Fig. 2b). The presence of noradrenaline and adrenaline was not observed in these cultures using an assay with a detection limit of 70 pg ml<sup>-1</sup> and 120 pg ml<sup>-1</sup> for noradrenaline and adrenaline, respectively.

To further characterize the dopamine-producing TH<sup>+</sup> neurons, semi-quantitative polymerase chain reaction with reverse transcription (RT-PCR) was used to evaluate expression of specific genes involved in dopamine neuron development and function. Nurr1, TH and aromatic L-amino acid decarboxylase (AADC) were all upregulated in differentiated Nurr1 ES cells compared with WT ES cells (Fig. 2c). Dopamine  $\beta$ -hydroxylase (DBH) and the transcription factor Phox2a, selective markers for adrenaline-mediated neurons, were not detected (data not shown). Treatment with Shh and FGF8 increased the expression of dopamine transporter (DAT),

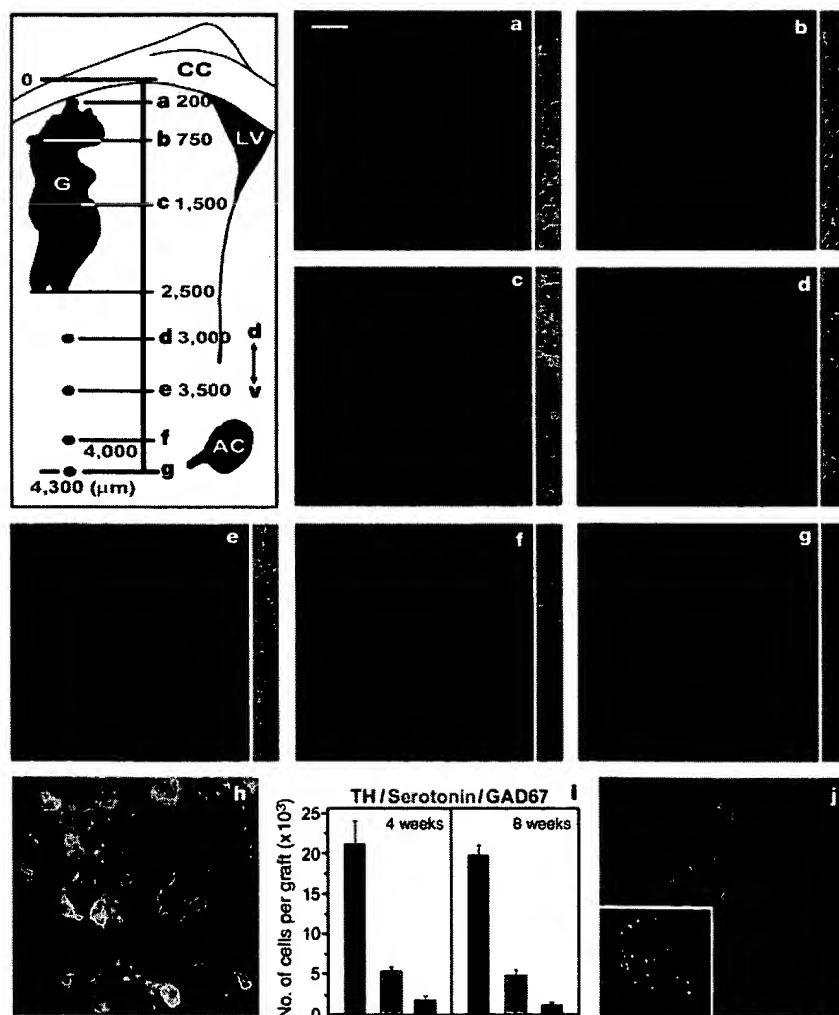


**Figure 3** Nurr1 ES cells integrate into the striatum of hemiparkinsonian rats. The diagram shows a drawing of a single section through a graft (G) in the striatum (LV, lateral ventricle; AC, anterior commissure). Single confocal images after immunohistochemistry for TH (red) are shown (a–g) from regions marked by red dots in the diagram. The distribution of cells and processes through the thickness of the section (35  $\mu$ m) is shown by the z-series displayed in green on the right. Note the many TH<sup>+</sup> processes that extend away from the

graft into the parenchyma of the host striatum (d–f). Scale bar, 50  $\mu$ m.

**h**, Immunoreactivity for the mouse-specific antigen M2 (green) and for TH (red, or yellow where it overlaps green) in the dorsal striatum of grafted animals. **i**, Survival of TH<sup>+</sup>, serotonin<sup>+</sup> and GAD67<sup>+</sup> cells in grafts at 4 and 8 weeks after transplantation. **j**, Lack of immunostaining for Ki-67 (green) in a graft (M2, red). Inset shows Ki-67 staining of a rat brain section containing glioma cells as a positive control.

**Table 1 Electrophysiological characterization of TH<sup>+</sup> neurons**

	TH <sup>+</sup> [A]	TH <sup>+</sup> (graft) [B]	TH <sup>+</sup> (host) [C]
Resting membrane potential (mV)*	-64 ± 3.5 (15) <sup>C</sup>	-67 ± 2.9 (21)	-77 ± 1.6 (19) <sup>A</sup>
Rectifier ratio (early/late)*	0.81 ± 0.05 (15) <sup>B,C</sup>	0.97 ± 0.02 (20) <sup>A</sup>	0.99 ± 0.03 (17) <sup>A</sup>
Action potential duration (ms)*	2.23 ± 0.17 (15) <sup>C</sup>	1.47 ± 0.24 (20)	1.1 ± 0.21 (17) <sup>A</sup>
Action potential amplitude (mV)	60 ± 2.1 (15)	57 ± 3.2 (20)	62 ± 2.2 (17)
Current–frequency relation (Hz pA <sup>-1</sup> )*	0.18 ± 0.11 (13) <sup>B,C</sup>	0.98 ± 0.14 (20) <sup>A</sup>	1.3 ± 0.21 (15) <sup>A</sup>
Maximum firing frequency (Hz)*	47 ± 8.4 (11) <sup>B,C</sup>	69 ± 6.5 (20) <sup>A</sup>	81 ± 6.7 (15) <sup>A</sup>

Characteristics of TH<sup>+</sup> versus TH<sup>+</sup> neurons *in vivo*. There are several properties of TH<sup>+</sup> neurons, characteristic of dopamine neurons, that are significantly different from those of TH<sup>+</sup> neurons. These differences are phenotype dependent, regardless of the origin of the cell—that is, host derived rather than ES cell derived. Data are presented as mean ± s.e.m. The number in parentheses is the number of cells for each value. Letters in brackets represent the different groups.

\**P* ≤ 0.025 by analysis of variance. A superscript letter denotes that the value is significantly different from the indicated group, using Tukey's post-hoc analysis.

which in vertebrates is exclusively found in dopamine neurons (Fig. 2c). The homeobox gene Ptx3, uniquely found in midbrain dopamine neurons<sup>25</sup>, was highly expressed in cultures of Nurr1 ES cells in the presence of Shh and FGF8 (Fig. 2c). A high level of En-1 messenger RNA was also found in Shh/FGF8-treated cells, suggesting that exposure of precursor cells to specific factors regulates gene expression at later stages of neuronal differentiation. These results are strong evidence that TH<sup>+</sup> cells generated from Nurr1 ES cells express many molecular, morphological and functional features expected of midbrain dopamine neurons.

We next explored the ability of differentiated WT and Nurr1-transfected ES cells to survive, integrate, and function in host animals. In rodents, administration of 6-hydroxy dopamine (6-OH-DA) in the striatum kills dopamine neurons, providing a useful model of Parkinson's disease. Animals lesioned with 6-OH-DA either received a sham operation or a graft of 5 × 10<sup>5</sup> Nurr1 ES cells (day 3 of stage 5). The sham-grafted animals showed no TH<sup>+</sup>

elements in the ipsilateral substantia nigra or the striatum. Animals grafted with Nurr1 ES cells were used for morphological analysis by TH immunostaining. All grafts were easily detected in the dorsal striatum by staining for the mouse-specific surface antigen M2 and for TH. TH<sup>+</sup> cells in the grafts show complex morphologies (Fig. 3a–c) and are positive for the calcium-binding protein calbindin (relative molecular mass 28,000), which is normally expressed in a subset of midbrain dopamine neurons that project to the striatum<sup>26</sup> (data not shown). In serial sections, the grafts were found to extend across 2.5 mm of the host striatum. TH<sup>+</sup> cell bodies were restricted to the region of the graft (Fig. 3a–c) but TH<sup>+</sup> processes were found in the parenchyma of the host striatum up to 2 mm from the graft (Fig. 3d–g). Many of the M2<sup>+</sup> grafted cells also expressed TH (Fig. 3h). To characterize the phenotype of grafted cells, we measured the number of neurons positive for TH, serotonin and glutamate decarboxylase (GAD67) in grafts at 4 and 8 weeks after implantation. None of the serotonin<sup>+</sup> or GAD67<sup>+</sup> neurons co-

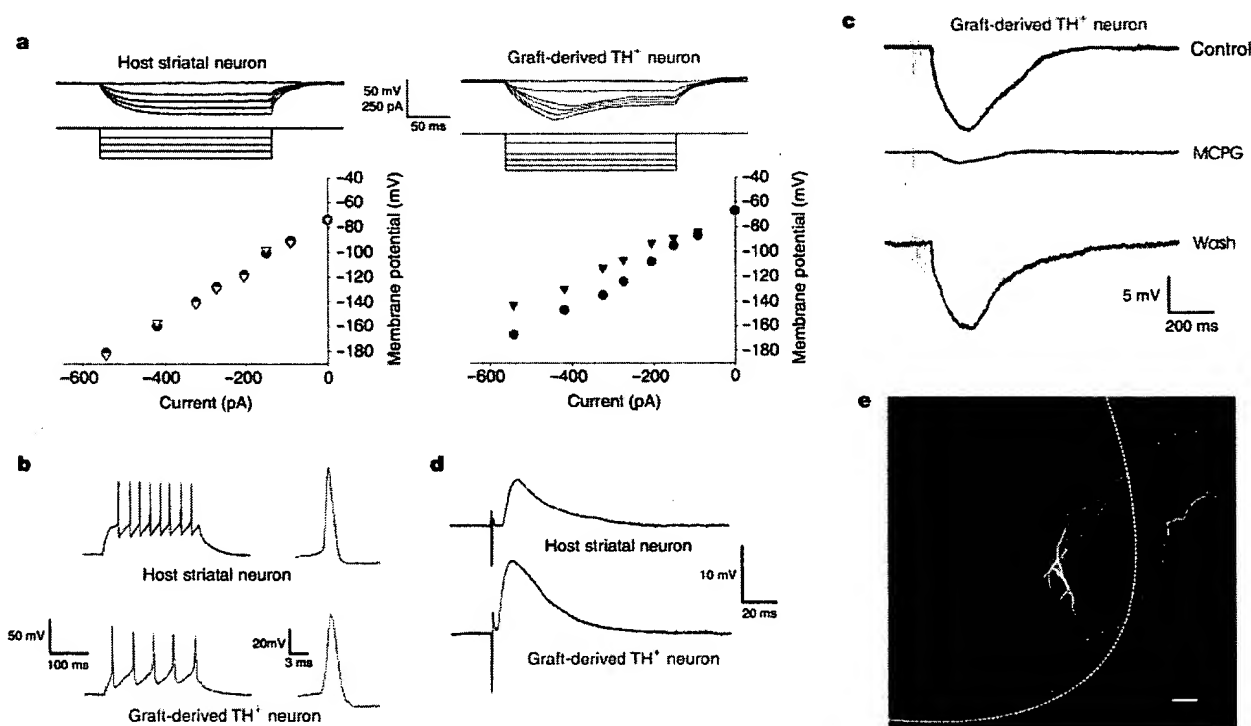


**Figure 4** Electrophysiological properties of TH<sup>+</sup> neurons. Simultaneous recordings were performed from neurons in the graft located on the graft–host border and neurons in the host striatum. **a**, Representative current–voltage relationship for a host striatal TH<sup>-</sup> neuron and a TH<sup>+</sup> neuron in the graft. The TH<sup>+</sup> neurons display the time-dependent anomalous rectifier characteristic of dopamine-synthesizing cells after a hyperpolarizing pulse. Circles, the full extent of the immediate reduction in the membrane potential; triangles, the sustained membrane potential. **b**, Spike train profiles of a host striatal neuron and a graft-derived TH<sup>+</sup> neuron. TH<sup>+</sup> neurons fired broader action potentials at a

lower frequency than TH<sup>-</sup> neurons. **c**, ES-derived TH<sup>+</sup> neurons in the graft displayed a unique evoked IPSP mediated by activation of the metabotropic glutamate receptors. **d**, Extracellular stimulation in the centre of the graft resulted in an EPSP in both a graft-derived TH<sup>+</sup> neuron and a host striatal neuron, indicating the presence of graft-to-host and graft-to-graft synapses. **e**, Confocal micrograph illustrating a biocytin-filled (green) TH<sup>+</sup> neuron in the graft in close proximity to other non-filled, graft-derived TH<sup>+</sup> neurons (red). The neuron was filled during recording. The filled neuron extends processes well into the host striatum. The dotted line shows the host–graft interface. Scale bar, 50 μm.

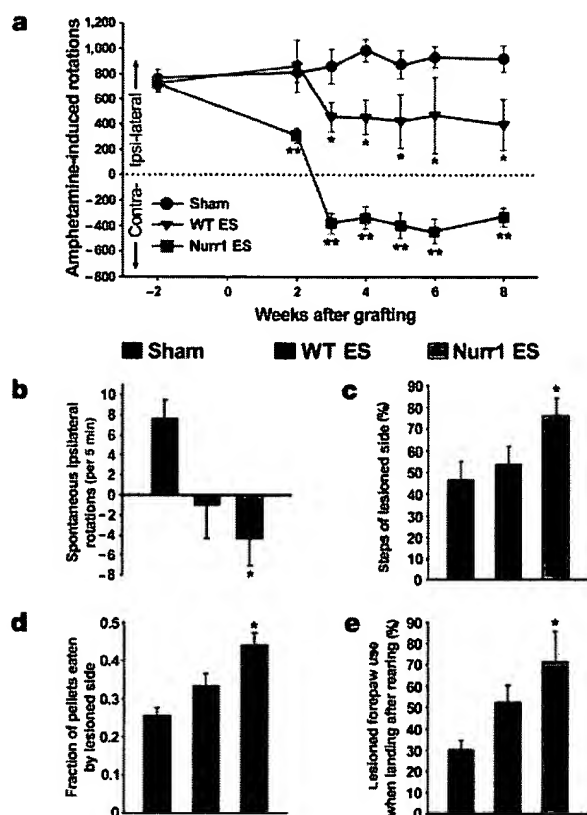


**Figure 5** Behavioural effects of grafted Nurr1 ES cells. **a**, Analysis of amphetamine-stimulated rotations in animals grafted with neurons derived from wild-type (WT) ( $n = 10$ ) or Nurr1 ES cells ( $n = 15$ ) and sham controls ( $n = 18$ ). **b–e**, Non-pharmacological evaluation of the animals grafted with either WT or Nurr1 ES cells (mean  $\pm$  s.e.m.). **b**, Nine weeks after grafting and one week after the last injection of amphetamine, spontaneous turning behaviour was evaluated for 5 min. **c**, The results in the adjusting step test are expressed as a percentage of the lesioned side relative to the number of steps with the non-lesioned paw. **d**, In the paw-reaching test, the number of pellets eaten with the lesioned paw were normalized by the total number of pellets eaten during the 7-day test period. **e**, In the cylinder test, the use of each limb was measured when rearing and landing. The percentage of use of the lesioned-side limb relative to the total number of landings after rearing is expressed. Asterisk,  $P < 0.05$ ; double asterisk,  $P < 0.001$ , compared with sham group.

expressed TH (data not shown). The great majority of neurons were TH<sup>+</sup> and neuron number did not change significantly between 4 and 8 weeks (Fig. 3i). The stability of cell number in the graft is also an important issue because undifferentiated ES cells cause teratomas. The expression of Ki-67, a characteristic antigen found in dividing cells, was used to search for cell proliferation in the graft. No Ki-67<sup>+</sup> cells were seen in the grafts (Fig. 3j) but they were abundant in sections of human glioma cells grafted into the adult rat brain (Fig. 3j, inset). Consistent with this finding, no teratomas were observed in animals that had received grafts of Nurr1 ES cells.

To test the electrophysiological properties of grafted neurons *in vivo*, rats were euthanized at several time points, up to 140 days after grafting, and brain slices (300  $\mu$ m thick, and containing the entire graft) were prepared for electrophysiological analysis. Using an infrared differential interference contrast (IR-DIC) microscope, neurons at the host-graft interface were preferentially targeted for recording. The properties of the recorded cells (Table 1) demonstrate that grafted TH<sup>+</sup> cells display electrophysiological characteristics similar to those of mesencephalic neurons<sup>27,28</sup>. For example, TH<sup>+</sup> neurons subjected to hyperpolarizing voltage steps showed anomalous rectification *in vivo* (Fig. 4a). TH<sup>+</sup> cells also showed

action potential frequency and duration properties distinct from TH<sup>−</sup> neurons in the graft and in the parenchyma of the host striatum (Fig. 4b and Table 1). These differences are similar to previous reports comparing TH<sup>+</sup> and TH<sup>−</sup> mesencephalic neurons<sup>27,28</sup>.

Mesencephalic dopamine neurons show a unique inhibitory postsynaptic potential (IPSP)<sup>29</sup>. In five of six grafted TH<sup>+</sup> neurons, a train of extracellular stimuli elicited this IPSP, which is dependent on metabotropic glutamate receptor type 1 (mGluR1) (Fig. 4c). In contrast, none of the five TH<sup>−</sup> neurons showed this IPSP. Simultaneous recordings were performed from medium spiny neurons in the host striatum and from candidate TH<sup>+</sup> neurons in the graft (Fig. 4d). Of 25 pairs of cells recorded, little or no spontaneous activity was observed and no direct synaptic connections were seen. However, when applying extracellular stimulation to a population of cells within the graft, excitatory postsynaptic potentials (EPSPs) were recorded in neurons both in the graft and in surrounding host cells up to 0.8 mm from the graft border (Fig. 4e). These results indicate that the ES-derived neurons develop functional synapses and show electrophysiological properties expected of mesencephalic neurons.

We next tested the behaviour of sham-operated animals and animals grafted with dopamine neurons differentiated to day 3 of stage 5. Amphetamine stimulation to animals lesioned unilaterally with 6-OH-DA induces a movement bias ipsilateral to the injection site. The sham group of animals showed a stable rotational bias (Fig. 5a). Animals grafted with  $5 \times 10^5$  cells derived from WT ES cells showed a slight recovery in rotation behaviour. In contrast, the group grafted with Nurr1 ES cells showed a marked change in this parameter leading to consistent contralateral turning (Fig. 5a). The turning biases were preserved in sham grafted groups and groups grafted with Nurr1 ES cells when spontaneous rotations were measured (Fig. 5b). In addition, the recovery of these animals was evaluated with a battery of non-pharmacological tests that provide a more direct measure of motor deficits analogous to those found in human Parkinson's disease. We observed a significant improvement in the Nurr1 group in the adjusting step, cylinder and paw-reaching tests (Fig. 5c–e). Anatomical analysis showed that dopamine neurons were present in all the animals grafted with neurons derived from WT and Nurr1-expressing ES cells. Further studies are required to determine the relationship between the number of dopamine neurons and the behavioural response. However, the recovery observed in the behavioural tests shows that neurons derived from Nurr1 ES cells function in response to both pharmacological stimulation and also in spontaneous integrative tasks.

## Discussion

The low efficiency of generation of dopamine neurons from primary cultures of fetal, neonatal cells or adult stem cells limits their therapeutic potential as donor cells. We report here that ES cells can efficiently generate midbrain precursors and dopamine neurons. The functional analysis of the ES-cell-derived neurons was conducted by anatomical, neurochemical, electrophysiological and behavioural tests. ES-cell-derived TH<sup>+</sup> cells release dopamine, extend axons into the host striatum, form functional synaptic connections and modulate spontaneous and pharmacologically induced behaviours. Grafted fetal midbrain-specific dopamine neurons innervate the striatum and improve motor asymmetry<sup>1,30,31</sup>. In contrast, hypothalamic dopamine neurons or nor-adrenaline neurons, which also express TH, did not innervate the striatum in a rat model of Parkinson's disease<sup>32–34</sup>. Our data support the notion that ES-cell-derived neurons survive and function after grafting into the lesioned striatum.

Although the results presented here encourage the development of strategies involving neurons derived from ES cells in the treatment of neurological disease, further studies are needed both in rodent and primate systems to address the long-term safety and efficacy of these cells. Inappropriate cells may be included along

with the midbrain dopamine neurons. For example, tumour formation is a problem associated with ES cell grafting in models of Parkinson's disease<sup>35</sup>. Under our conditions, differentiated neurons were enriched and dividing cells were not seen in a series of grafts that were analysed up to 8 weeks after transplantation; however, additional long-term data are needed to show that ES-derived cells do not divide *in vivo*. The dopamine and serotonin neurons of the mid- and hindbrain are also important in mood disorders and schizophrenia<sup>36,37</sup>. Our results justify the continued study of the therapeutic benefits that can be derived from the use of ES cells, with the ultimate goal being the successful application of therapies based on ES cells in the treatment of neurological and psychiatric disease. □

## Methods

### Generation of Nurr1 ES cells and differentiation

A full-length cDNA fragment for rat Nurr1 was cloned into pCMV $\beta$  vector (Clontech) by replacing  $\beta$ -galactosidase with a HA-tagged Nurr1 cDNA (HA-Nurr1) generated by fusing the HA tag (YPYDVPDYA) in frame at the 5' end to the Nurr1 cDNA. Mouse ES cells (R1) were co-transfected with pCMV-HA-Nurr1 and the neomycin resistance plasmid (pCDNA3.1; Invitrogen) by electroporation (0.25 kV, 500  $\mu$ F), and transfected clones were selected by growth in the presence of G418 (200  $\mu$ g ml<sup>-1</sup>). The selected clones were screened for expression of HA-Nurr1 by immunoblot analysis, and five clones showing the highest levels of expression were chosen for differentiation experiments. Wild-type R1 ES cells were used as controls. To induce differentiation, ES cells were cultured as described<sup>8</sup> or processed with Mouse Dopaminergic Neuron Differentiation Kit (R&D Systems) except for treatment with LIF at stage 2, during embryoid body (EB) formation.

### Immunostaining of cultured cells and cryosections

Cultured cells were fixed in 4% paraformaldehyde in PBS. Perfused brain tissue was soaked in 20% sucrose overnight, frozen in isopentane cooled by solid CO<sub>2</sub> and cut on a cryostat at 35  $\mu$ m. The following antibodies were used: En-1, 1:50; M2, 1:100 (monoclonal, all from Developmental Studies Hybridoma Bank); Otx2 polyclonal<sup>38</sup>, 1:1,000 (provided by G. Corte), Bf1 polyclonal<sup>39</sup>, 1:1,000 (provided by E. Lai), Pax-2 polyclonal, 1:200 (Covance); TH polyclonal, 1:400 (PelFreeze), or monoclonal, 1:1,000 (Sigma); serotonin polyclonal, 1:4,000 (Sigma); HA monoclonal, 1:200 (Santa Cruz Biotechnology); Nurr1 monoclonal, 1:1,000 (BD Transduction Laboratories); GAD67 polyclonal, 1:1,000 (Chemicon); and Ki-67 polyclonal, 1:200 (Novocastra). Appropriate fluorescence-tagged (Jackson ImmunoResearch Laboratories) or biotinylated (Vector Laboratories) secondary antibodies were used for visualization. Specimens were examined on Zeiss Axioplan or Zeiss LSM 510 confocal imaging system. Stacked optical sections were merged using Maximum Projection software (Zeiss). Quantitative immunocytochemical data were expressed as means  $\pm$  s.e.m.

### Reverse-phase HPLC determinations of catecholamine

Catecholamine levels were determined after 15 days of differentiation. Dopamine release was stimulated in Hank's balanced salt solution (HBSS) containing 56 mM KCl (evoked release, 15 min incubation). Dopamine extraction and HPLC analysis have been described previously<sup>1</sup>.

### RT-PCR and immunoblot analysis

Total cellular RNA purification and RT-PCR was carried out as previously described<sup>8</sup>. The following primers were used to amplify target cDNA: Nurr1, 5'-TAAAGGCCGAGAGGTCGTC-3' and 5'-CTCTCTTGGTTCCTTGAGCC-3'; TH, 5'-CTCCTTGTCTCGGGCTGTA-3' and 5'-CTGAGCTTGTCTTGGCGTCA-3'; Ptx3, 5'-AGGACGGCTCTCTGAAGAA-3' and 5'-TTGACCGAGTTGAAGGCCAA-3'; En-1, 5'-TCAAGACTGACTCACAGCAACCCC-3' and 5'-CTTTGTCTGAACCGTGGTGGTAG-3'; c-RET, 5'-GGCCCGGAGTGTGAGGAATGTG-3' and 5'-GCTGATGCAATGGGCGGCTGTGC-3'; DAT, 5'-GGACCAATGTCTTCAGTGGTGGC-3' and 5'-GGATCCATGGGAGGTCCATGG-3'; AADC, 5'-CCTACTGGTCTCGGACTAA-3' and 5'-GGCTACCACTGACTCAAACTC-3'; Phox2a, 5'-TGGCGCTCAAGATCGACCTCA-3' and 5'-CGTTAGGGTGGGATTAGCGGT-3'; DBH, 5'-TTCCAATGTGCAGCTGAGTC-3' and 5'-GGTGCACCTTGTCTTGTGAGT-3'; GAPDH, 5'-ACCACAGTCCATGCCATCAC-3' and 5'-TCCACCACCTCTTGTCTGA-3'. Immunoblot analysis was performed as previously described<sup>39</sup>.

### Electrophysiology

Striatal slices (coronal, 300  $\mu$ m) were prepared and recordings were performed as previously reported<sup>40</sup>. Briefly, grafted animals were euthanized at time points from 30 to 140 d after grafting, and slices were recorded in a submerged slice chamber at 30–32 °C, superfused at a rate of  $\sim$ 2 ml min<sup>-1</sup> with artificial cerebrospinal fluid (ACSF). Extracellular stimulation was delivered through a bipolar stainless steel electrode. For recording of the mGluR1-mediated IPSPs, slices were bathed in ACSF containing picrotoxin (100  $\mu$ M), strychnine (1  $\mu$ M), eticlopride (100 nM), CNQX (25  $\mu$ M) and saclofen (10  $\mu$ M), as described<sup>29</sup>.

Biocytin (0.2%) was added to the intracellular medium daily. Recordings were performed under visual guidance using an upright microscope. Voltage clamp recordings were performed at holding potentials of  $-60$  to  $-70$  mV, signals were

amplified using an Axopatch 200B amplifier, current clamp recordings were performed with a second amplifier (AxoClamp 2B), and all data were acquired and analysed on a PC running pClamp 8 (Axon Instruments). Drugs were applied by perfusion.

### Transplantation and behavioural testing

Adult female Sprague-Dawley rats lesioned with 6-OH-DA were purchased (Taconic Farms). All surgical procedures were done according to guidelines of the National Institutes of Health (NIH) and National Institute of Neurological Disorders and Stroke (NINDS). WT and Nurr1 ES cells were trypsinized at day 3 of stage 5, and re-suspended at a density of 160,000 viable cells per  $\mu$ l. Three microlitres of the cell suspension were grafted into the lesioned striatum of hemiparkinsonian rats (0.0 mm anteroposterior, +3.0 mm mediolateral and  $-5.0$  mm dorsoventral of bregma and the meninges). In sham animals, 3  $\mu$ l of N2 medium was injected. The number of animals studied were: sham, 18; WT, 10; and Nurr1, 15. All animals were immunosuppressed with cyclosporine A (Neoral, Novartis, 10 mg kg<sup>-1</sup> d<sup>-1</sup>, intraperitoneally, i.p.) starting 24 h before grafting. Amphetamine-induced (2.5 mg kg<sup>-1</sup>, i.p.) rotational behaviour was evaluated for 70 min as described<sup>1</sup>, before and after ES cell grafting, in animals with stable scores of  $>6$  ipsilateral turns per min. To quantify neuronal survival after grafting, immunohistochemical analysis was performed 4 and 8 weeks after grafting in the Nurr1 group. Several non-pharmacological tests were done as described, starting 9 weeks after grafting, as follows. (1) Spontaneous rotations<sup>41</sup>. (2) Adjusting step test<sup>41</sup>. Animals were moved in the backhand direction by a blind experimenter. The test was made three times per session, two sessions per day during three consecutive days. The results are expressed as a percentage of steps in lesioned compared with non-lesioned sides. Number of adjusting steps with the non-lesioned paw were: sham, 13.2  $\pm$  0.3; WT, 13.0  $\pm$  0.3; Nurr1, 12.6  $\pm$  0.5. (3) Paw-reaching test. Animals were kept on a restricted diet until they lost 10–15% of their initial weight and then tested for 7 d in the appropriate chambers as described<sup>42</sup>. The results are given as the average fraction of pellets eaten by the lesioned side relative to the total number per day. In five naive animals, the fraction of pellets eaten by the right side was 0.51  $\pm$  0.02. (4) Cylinder test<sup>43</sup>. An observer, blind to the treatment, quantified two parameters: the number of wall contacts with each forelimb when rearing, and the number of times the rat used either forelimb for landing in at least 15 rearing-landing cycles. We expressed data as the percentage of use of the lesioned forepaw. For rearing, the percentages of contacts with the lesioned limb relative to the total number of contacts were not statically different between groups: sham, 4.4%  $\pm$  2.4; WT, 4.6%  $\pm$  5.2; Nurr1, 31.9%  $\pm$  20.0. For landing, the animals used almost always the non-lesioned paw either alone or together with the lesioned limb (sham and WT animals used the non-lesioned limb 100% of the time and Nurr1 used it 91.7  $\pm$  8.3%). The significant increase ( $P < 0.05$  relative to sham animals) in use of the lesioned side by the Nurr1 animals correlated with a significant decrease ( $P < 0.05$ ) in the exclusive use of the non-lesioned paw. For these non-pharmacological tests, we studied five sham-operated, four WT and four Nurr1-grafted rats, in which the presence of dopamine neurons was also confirmed in the grafts. In all experiments, mean  $\pm$  s.e.m. is represented. Statistical analysis was done by analysis of variance (ANOVA) followed by Fisher's test.

Received 24 April; accepted 12 June 2002; doi:10.1038/nature00900.

Published online 20 June 2002.

1. Studer, L., Tabar, V. & McKay, R. D. Transplantation of expanded mesencephalic precursors leads to recovery in parkinsonian rats. *Nature Neurosci.* **1**, 290–295 (1998).
2. Sanchez-Pemate, R., Studer, L., Bankiewicz, K. S., Major, E. O. & McKay, R. D. *In vitro* generation and transplantation of precursor-derived human dopamine neurons. *J. Neurosci.* **Res.** **65**, 284–288 (2001).
3. Thomson, J. A. *et al.* Embryonic stem cell lines derived from human blastocysts. *Science* **282**, 1145–1147 (1998).
4. Shamblo, M. J. *et al.* Derivation of pluripotent stem cells from cultured human primordial germ cells. *Proc. Natl Acad. Sci. USA* **95**, 13726–13731 (1998).
5. McDonald, J. W. *et al.* Transplanted embryonic stem cells survive, differentiate and promote recovery in injured rat spinal cord. *Nature Med.* **5**, 1410–1412 (1999).
6. Rideout, W. M. III, Hochedlinger, K., Kyba, M., Daley, G. & Jaenisch, R. Correction of a genetic defect by nuclear transplantation and combined cell and gene therapy. *Cell* **109**, 17–27 (2002).
7. Kyba, M., Perlingeiro, R. C. R. & Daley, G. Q. HoxB4 confers definitive lymphoid–myeloid engraftment potential on embryonic stem cell and yolk sac hematopoietic progenitors. *Cell* **109**, 29–37 (2002).
8. Lee, S. H., Lumelsky, N., Auerbach, J. M. & McKay, R. D. Efficient generation of midbrain and hindbrain neurons from mouse embryonic stem cells. *Nature Biotechnol.* **18**, 675–679 (2000).
9. Okabe, S., Forsberg-Nilsson, K., Spiro, A. C., Segal, M. & McKay, R. D. Development of neuronal precursor cells and functional postmitotic neurons from embryonic stem cells *in vitro*. *Mech. Dev.* **59**, 89–102 (1996).
10. Wallen, A. *et al.* Fate of mesencephalic AHD2-expressing dopamine progenitor cells in NURR1 mutant mice. *Exp. Cell Res.* **253**, 737–746 (1999).
11. Zetterstrom, R. H. *et al.* Dopamine neuron agenesis in Nurr1-deficient mice. *Science* **276**, 248–250 (1997).
12. Saucedo-Cardenas, O. *et al.* Nurr1 is essential for the induction of the dopaminergic phenotype and the survival of ventral mesencephalic late dopaminergic precursor neurons. *Proc. Natl Acad. Sci. USA* **95**, 4013–4018 (1998).
13. Le, W. *et al.* Selective agenesis of mesencephalic dopaminergic neurons in Nurr1-deficient mice. *Exp. Neurol.* **159**, 451–458 (1999).
14. Lumelsky, N. *et al.* Differentiation of embryonic stem cells to insulin-secreting structures similar to pancreatic islets. *Science* **292**, 1389–1394 (2001).
15. Bader, A., Al-Dubai, H. & Weitzer, G. Leukemia inhibitory factor modulates cardiogenesis in embryoid bodies in opposite fashions. *Circ. Res.* **86**, 787–794 (2000).
16. Molne, M. *et al.* Early cortical precursors do not undergo LIF-mediated astrocytic differentiation. *J. Neurosci. Res.* **59**, 301–311 (2000).
17. Offield, M. F. *et al.* PDX-1 is required for pancreatic outgrowth and differentiation of the rostral



- duodenum. *Development* 122, 983–995 (1996).
18. Hynes, M. & Rosenthal, A. Specification of dopaminergic and serotonergic neurons in the vertebrate CNS. *Curr. Opin. Neurobiol.* 9, 26–36 (1999).
19. Wurst, W. & Bally-Cuif, L. Neural plate patterning: upstream and downstream of the isthmus organizer. *Nature Rev. Neurosci.* 2, 99–108 (2001).
20. Ye, W., Shimamura, K., Rubenstein, J. L., Hynes, M. A. & Rosenthal, A. FGF and Shh signals control dopaminergic and serotonergic cell fate in the anterior neural plate. *Cell* 93, 755–766 (1998).
21. Broccoli, V., Boncinelli, E. & Wurst, W. The caudal limit of Otx2 expression positions the isthmus organizer. *Nature* 401, 164–168 (1999).
22. Joyner, A. L., Liu, A. & Millet, S. Otx2, Gbx2 and Fgf8 interact to position and maintain a mid-hindbrain organizer. *Curr. Opin. Cell Biol.* 12, 736–741 (2000).
23. Tao, W. & Lai, E. Telencephalon-restricted expression of BF-1, a new member of the HNF-3/fork head gene family, in the developing rat brain. *Neuron* 8, 957–966 (1992).
24. Wurst, W., Auerbach, A. B. & Joyner, A. L. Multiple developmental defects in *Engrailed-1* mutant mice: an early mid-hindbrain deletion and patterning defects in forelimbs and sternum. *Development* 120, 2065–2075 (1994).
25. Smidt, M. P. *et al.* A second independent pathway for development of mesencephalic dopaminergic neurons requires *Lmx1b*. *Nature Neurosci.* 3, 337–341 (2000).
26. Gerfen, C. R., Baimbridge, K. G. & Thibault, J. The neostriatal mosaic: III. Biochemical and developmental dissociation of patch-matrix mesostriatal systems. *J. Neurosci.* 7, 3935–3944 (1987).
27. Reypert, S. *et al.* Identified postnatal mesolimbic dopamine neurons in culture; morphology and electrophysiology. *J. Neurosci.* 12, 4264–4280 (1992).
28. Rohrbacher, J., Ichinohe, N. & Kitai, S. T. Electrophysiological characteristics of substantia nigra neurons in organotypic cultures: spontaneous and evoked activities. *Neuroscience* 97, 703–714 (2000).
29. Fiorillo, C. D. & Williams, J. T. Glutamate mediates an inhibitory postsynaptic potential in dopamine neurons. *Nature* 394, 78–82 (1998).
30. Abrous, D. N., Shaltot, A. R., Torres, E. M. & Dunnett, S. B. Dopamine-rich grafts in the neostriatum and/or nucleus accumbens: effects on drug-induced behaviours and skilled paw-reaching. *Neuroscience* 53, 187–197 (1993).
31. Nikkha, G., Duan, W. M., Knappe, U., Jödicke, A. & Björklund, A. Restoration of complex sensorimotor behaviour and skilled forelimb use by a modified nigral cell suspension transplantation approach in the rat Parkinson model. *Neuroscience* 56, 33–43 (1993).
32. Zuddas, A., Corsini, G. U., Barker, J. L., Kopin, I. J. & di Porzio, U. Specific reinnervation of lesioned mouse striatum by grafted mesencephalic dopaminergic neurons. *Eur. J. Neurosci.* 3, 77–85 (1991).
33. Hudson, J. L., Bickford, P., Johansson, M., Hoffer, B. J. & Stromberg, I. Target and neurotransmitter specificity of fetal central nervous system transplants: importance for functional reinnervation. *J. Neurosci.* 14, 283–290 (1994).
34. Björklund, A. & Lindvall, O. Cell replacement therapies for central nervous system disorders. *Nature Neurosci.* 3, 537–544 (2000).
35. Björklund, L. M. *et al.* Embryonic stem cells develop into functional dopaminergic neurons after transplantation in a Parkinson rat model. *Proc. Natl Acad. Sci. USA* 99, 2344–2349 (2002).
36. Gross, C. *et al.* Serotonin1A receptor acts during development to establish normal anxiety-like behaviour in the adult. *Nature* 416, 396–400 (2002).
37. Sawa, A. & Snyder, S. H. Schizophrenia: diverse approaches to a complex disease. *Science* 296, 692–695 (2002).
38. Mallamaci, A., Di Blas, E., Briata, P., Boncinelli, E. & Corte, G. OTX2 homeoprotein in the developing central nervous system and migratory cells of the olfactory area. *Mech. Dev.* 58, 165–178 (1996).
39. Le, W. L., Conneely, O. M., He, Y., Jankovic, J. & Appel, S. H. Reduced *Nurr1* expression increases the vulnerability of mesencephalic dopamine neurons to MPTP-induced injury. *J. Neurochem.* 73, 2218–2221 (1999).
40. Auerbach, J. M., Eiden, M. V. & McKay, R. D. Transplanted CNS stem cells form functional synapses *in vivo*. *Eur. J. Neurosci.* 12, 1696–1704 (2000).
41. Olsson, M., Nikkha, G., Bentlage, C. & Björklund, A. Forelimb akinesia in the rat Parkinson model: Differential effects of dopamine agonists and nigral transplants as assessed by a new stepping test. *J. Neurosci.* 15, 3863–3875 (1995).
42. Montoya, C. P., Campbell, H. L., Pemberton, K. D. & Dunnett, S. B. The 'staircase test': a measure of independent forelimb reaching and grasping abilities in rats. *J. Neurosci. Methods* 36, 219–228 (1991).
43. Schallert, T., Fleming, S. M., Leasure, J. L., Tillerson, J. L. & Bland, S. T. CNS plasticity and assessment of forelimb sensorimotor outcome in unilateral rat models of stroke, cortical ablation, parkinsonism and spinal cord injury. *Neuropharmacology* 39, 777–787 (2000).

#### Acknowledgements

We thank J. Harvey-White for technical assistance with HPLC, P. Brasted for advice on the non-pharmacological evaluation of the grafted animals, and J. Kordower for supplying boxes for the paw-reaching test, E. Lai for the anti-bb1 antibody and G. Corte for the anti-OTX2 antibody. We thank D. Owens for critical discussion of the manuscript. J.A.R.-G. was supported by a postdoctoral fellowship from the Spanish Ministerio de Educación, Cultura y Deporte. I.V. is a Pew Latin American fellow. We thank the National Parkinson Foundation and the Tuchman Foundation for their support.

#### Competing interests statement

The authors declare that they have no competing financial interests.

Correspondence and requests for materials should be addressed to R.M. (e-mail: mckay@codon.nih.gov).